QUATERNARY RESEARCH 44, 341–354 (1995)

The GISP2 $\delta^{18}O$ Climate Record of the Past 16,500 Years and the Role of the Sun, Ocean, and Volcanoes

MINZE STUIVER, PIETER M. GROOTES,* AND THOMAS F. BRAZIUNAS

Department of Geological Sciences and Quaternary Research Center, University of Washington, Seattle, Washington 98195

Received April 24, 1995

Measured $^{18}O/^{16}O$ ratios from the Greenland Ice Sheet Project 2 (GISP2) ice core extending back to 16,500 cal yr B.P. provide a continuous record of climate change since the last glaciation. High-resolution annual $^{18}O/^{16}O$ results were obtained for most of the current millennium (A.D. 818–1985) and record the Medieval Warm Period, the Little Ice Age, and a distinct 11-yr $^{18}O/^{16}O$ cycle. Volcanic aerosols depress central Greenland annual temperature (~1.5°C maximally) and annual $^{18}O/^{16}O$ for about 4 yr after each major eruptive event. On a bidecadal to millennial time scale, the contribution of solar variability to Holocene Greenlandic temperature change is ~0.4°C. The role of thermohaline circulation change on climate, problematic during the Holocene, is more distinct for the 16,500–10,000 cal yr B.P. interval. (Analogous to ^{14}C age calibration terminology, we express time in calibrated (cal) yr B.P. (A.D. 1950 = 0 cal yr B.P.)). The Oldest Dryas/Bølling/Older Dryas/Allerød/Younger Dryas sequence appears in great detail. Bidecadal variance in $^{18}O/^{16}O$, but not necessarily in temperature, is enhanced during the last phase of lateglacial time and the Younger Dryas interval, suggesting switches of air mass transport between jet stream branches. The branched system is nearly instantaneously replaced at the beginning of the Bølling and Holocene (at ~14,670 and ~11,650 cal yr B.P., respectively) by an atmospheric circulation system in which $^{18}O/^{16}O$ and annual accumulation initially track each other closely. Thermodynamic considerations of the accumulation rate–temperature relationship can be used to evaluate the $^{18}O/^{16}O$–temperature relationship. The GISP2 ice-layer-count years of major GISP2 climate transitions also support the use of coral ^{14}C ages for age calibration.

INTRODUCTION

Ice cores, with their continuous diary of highly detailed physical and chemical properties, are natural recorders of climate change for ice age cycles. During the past decades, knowledge of abrupt switches, as well as seasonal to millennial trends, in climate has advanced dramatically. To add to this knowledge, we present a new GISP2 high-resolution $^{18}O/^{16}O$ ice core time series on an annual scale back to A.D. 818 and on a bidecadal time scale back to 16,500 cal yr B.P. The data provide information on conversion of isotope information to mean annual temperature change, Medieval warming, and Little Ice Age cooling in Greenland, and $^{18}O/^{16}O$ and accumulation variability during abrupt climate transitions. We also discuss causes of climate change, such as volcanic aerosols, solar output, oceanic thermohaline circulation, and air mass trajectories.

$\delta^{18}O$ AS A REGIONAL CLIMATE PARAMETER

To derive mean annual surface temperature (T) from Greenland ice core $\delta^{18}O$,[1] a spatially determined present-day $\delta^{18}O/T$ gradient of ~0.6‰ per °C (e.g., Dansgaard *et al.*, 1973) is usually applied. Nonspatial approaches, using borehole temperatures and brightness temperature trends, lead to similar gradients (Cuffey *et al.*, 1994; Shuman *et al.*, 1995) at the GISP2 site. The $\delta^{18}O/T$ paleo-gradient also depends on shifts in seasonal partitioning of precipitation amounts, or seasonal cycle $\delta^{18}O$ amplitude (Steig *et al.*, 1994; Hammer, 1982) as well as shifts in the water vapor source region (Charles *et al.*, 1994), air mass trajectories, or regional water vapor conditions (Whillans and Grootes, 1985). $\delta^{18}O$ "noise" levels in polar ice also are tied to microenvironmental climate variance, the degree of perturbation of annual snow layers prior to inclusion in the firn (i.e., snow drifting), and water vapor transport in snow and/or firn.

Locally added $\delta^{18}O$ variance is evident from a study of Clausen *et al.* (1988), who found intercore $\delta^{18}O$ correlation coefficients averaging only 0.40 ± 0.18 for a series of Greenland cores 25- to 100-m-long (up to 360 yr of ice accumulation, 70.6–71.5°N, 320.4–324.2°E). Similarly, when comparing GISP2 δD isotopic records with 110-yr temperature data from the west and east coast of Greenland, Baffin Island, and Iceland, Barlow (1994) noticed variable correlation coefficients ($r \sim 0.4$ to 0.7) between the records both for seasonal and longer time resolution.

Regional climate changes on a millennial time scale are more dependably recorded. The low-resolution $\delta^{18}O$ profiles of the ~3000-m-long GISP2 and Greenland Ice-Core Project

* Present address: C-14 Laboratory of the Christian Albrechts Universität Kiel, Leibnizstrasse 19, Kiel, Germany.

[1] $\delta^{18}O$, defined relative to standard mean ocean water (V-SMOW), equals $[(^{18}O/^{16})_{sample}-(^{18}O/^{16}O)_{SMOW}/(^{18}O/^{16}O)_{SMOW}]1000‰$.

0033-5894/95 $12.00

(GRIP) cores (drilled 28 km apart near 72.58°N, 38.48°W) correlate with an r value of 0.95 for the 10,000–100,000 cal yr B.P. interval (Grootes *et al.,* 1993). For the entire Holocene interval (and bidecadal time resolution), regional climate forcing also is a major player because Holocene $\delta^{18}O$ of both cores have about 60% of their variance in common ($r = 0.76$). However, r values drop to 0.54 and 0.23, respectively, for century (5-point moving average) and bidecadal variability when using the 2000–9000 cal yr B.P. interval (with fairly stable average $\delta^{18}O$). The bidecadal r value is preliminary because an estimated Holocene GRIP time scale was used (a "final" time scale not yet being available to us).

Clearly Holocene annual, decadal, or century type climate variability derived from ice core $\delta^{18}O$ (e.g., mean annual temperature) represents regional climate to a limited degree only. Nevertheless, the record is only partially adulterated by "extraneous" noise and valuable information can still be obtained.

MEASUREMENT OF $\delta^{18}O$ AND SUBSEQUENT CORRECTIONS

Mass spectrometric $\delta^{18}O$ reproducibility (one standard deviation, σ) is 0.04‰. Additional variance relates to the isotopic equilibration of the CO_2 gas and sample water at a constant temperature. We included in each batch of 10 water samples an aliquot of an Antarctic standard water to detect any possible offsets in $\delta^{18}O$ results. In 9 out of 10 cases there were no detectable offsets, and here the $\delta^{18}O$ average is −33.4641‰ (based on 6316 $\delta^{18}O$ Antarctic standard water determinations over 14 yr, with only 3 outlyers being rejected). The single measurement σ is 0.140‰. When including the off-set corrected data, $\sigma = 0.142$‰.

The water samples were stored in high-density polyethylene bottles, of which a small number were initially tested for water vapor permeability at room temperature over intervals of several weeks. This testing did not show any measurable sample $\delta^{18}O$ change. The majority of the samples were stored frozen at −12°C. Relative to samples stored at room temperature, water vapor exchange should be at least 10 times less in the cold room.

Due to the occasional lack of cold room space, a portion of the samples was stored for extended time intervals (up to 2 yr) at room temperature. For these samples, we found subsequently that minor $\delta^{18}O$ enrichment had taken place. However, $\delta^{18}O$ values of samples stored frozen for several years were unchanged.

A major complication was a change in properties of polyethylene bottles received in 1992. The supplier of the bottles did not inform us of these changes, and differences were not noticed in the field (the bottles were identical to the previous ones in outside dimensions and the texture of the plastic was the same). Nevertheless, the wall was about 30% thinner and the chemical composition of the plastic may have changed as well. For these thin-walled bottles we find very large $\delta^{18}O$ increases for samples stored at room temperature. There is also a significant relationship (Fig. 1) between the $\delta^{18}O$ increases and the amounts of water remaining in the sample bottles (in the field the bottles were filled with approximately equal amounts of water). The dashed line in Figure 1 depicts the calculated $\delta^{18}O$ enrichment due to water vapor loss (diffusion through the walls). As the observed enrichment is about double the calculated one, a second mechanism has to play a role. We suggest vapor exchange through "pumping," e.g., each time the barometric pressure increases, water vapor in the storage room (which has a $\delta^{18}O$ value much higher than that of polar water) diffuses into the sample bottle and equilibrates with the remaining sample. Pumping and diffusive losses evidently contributed about equally to the $\delta^{18}O$ enrichment.

As the $\delta^{18}O$ enrichment in the thin-walled bottles is very substantial, we rejected all results obtained for waters stored in thin-walled bottles. However, for samples stored at room temperature in regular polyethylene bottles the $\delta^{18}O$ changes are small. Here we derived a $\delta^{18}O$ enrichment correction from the step changes in average $\delta^{18}O$ measured for sample batches with different storage time. Based on these observations, measured $\delta^{18}O$ values were corrected for room temperature storage time. The ultimate corrections (Table 1) apply to samples between 751 and 1600 m depth in the core and range from 0.0‰ to a maximum of 0.64‰ for samples stored at room temperature for nearly 2 yr. In only one instance, for 1-m samples between 1543 and 1588 m, our information was insufficient for the calculation of a storage correction, and here we based the adjustment on the average offset with GRIP core data.

The corrections reduce the stated measuring precision of 0.14‰ to some extent. The overall deterioration in precision, however, is fairly small as can be seen from the similar GRIP and GISP2 σ's of, respectively, 0.31 and 0.38‰ for bidecadal $\delta^{18}O$ over the 2000–9000 cal yr B.P. interval. The offset between the average GISP2 and GRIP (Dansgaard *et al.,* 1993) $\delta^{18}O$ values is 0.10‰ for the full Holocene.

$\delta^{18}O$ storage corrections were not needed for samples stored at −12°C in regular polyethylene bottles. For instance, none of the single-year $\delta^{18}O$ values had to be adjusted.

ANNUAL (A.D. 818–1985) AND BIDECADAL $\delta^{18}O$ TIME SERIES

Samples were collected with sufficient density to obtain information on seasonal (monthly) $\delta^{18}O$ change for most of the

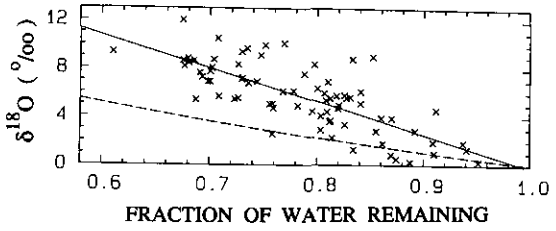

FIG. 1. Storage-related $\delta^{18}O$ enrichment (crosses) of water samples at room temperature versus fraction of water remaining in thin-walled polyethylene bottles. Solid line depicts linear correlation between the variables ($r = -0.74$) whereas the dashed line represents the calculated enrichment through Raleigh distillation.

TABLE 1
GISP2 Holocene $\delta^{18}O$ Corrections to Grootes *et al.* (1994)

The following storage enrichment corrections were deducted from measured $\delta^{18}O$ values:

- 0.30‰ from 751.52 to 779.44 m (3484 to 3648 yr B.P.)
- 0.30‰ from 834.13 to 1370.73 m (3980 to 8018 yr B.P.)
- 0.30‰ from 1510.18 to 1516.60 m (9376 to 9445 yr B.P.)
- 0.22‰ from 1516.60 to 1518.6 m (9445 to 9466 yr B.P.)
- 0.52‰ from 1518.6 to 1522.96 m (9466 to 9517 yr B.P.)
- 0.58‰ from 1522.96 to 1542.94 m (9517 to 9747 yr B.P.)
- 0.64‰ from 1543.00 to 1588.00 m (9748 to 10,286 yr B.P.)
- 0.12‰ from 1588.00 to 1600.00m (10,286 to 10,443 yr B.P.)

record. Although $\delta^{18}O$ of precipitation changes seasonally, annual ice layers identified by visual stratigraphy do not always contain a seasonal $\delta^{18}O$ imprint due to the isotopic modification caused by snow mixing, vapor diffusion, and ice flow (thinning). Yearly averaging yielded the $\delta^{18}O$ profiles (A.D. 818–1985) of Figure 2. The adopted time scale, with an estimated error of up to 2% (Meese *et al.*, 1994a), is based on annual layer counts. Because ice layer count years are bracketed by summer layers, specific A.D. years run from the summer of the preceding year to the summer of the actual year.

Figure 3 depicts the 100-yr moving averages of the highest and lowest $\delta^{18}O$ values encountered for each year, together with the actual $\delta^{18}O$ differences (expressed as $\Delta\delta^{18}O$) between both curves. The seasonal $\delta^{18}O$ signal is attenuated considerably in the firn due to water vapor diffusion (Johnsen and Robin, 1983). The attenuation is especially noticeable for the post-A.D. 1800 interval (Fig. 3), where summer and winter $\delta^{18}O$ trends widen drastically (the firn–ice boundary is at ~85 m or about A.D. 1735). Prior to A.D. 1800, $\Delta\delta^{18}O$ varies on century time scales, rather than showing a monotonic decrease with age, which suggests that these variations reflect actual changes in summer–winter contrast. The 1.0 and 0.8‰ reduction in summer and winter $\delta^{18}O$ values, respectively, between A.D. 975 and A.D. 1720 signals the climate change from the highs of Medieval warming (Medieval Warm Period or MWP) to the lows of Little Ice Age (LIA) cooling. The A.D. 1720 date falls within the A.D. 1570–1730 interval characterized by the lowest Northern Hemispheric summer temperatures of the last 500 yr (Bradley and Jones, 1993). Summer–winter $\delta^{18}O$ contrast is strongest (2.0‰) near the MWP maximum around A.D. 975 and lowest (1.6‰) near the start of the LIA at about A.D. 1450. The MWP and LIA intervals are, respectively, ~A.D. 900–1350 and ~A.D. 1350–1800 (Figs. 2 and 4). Mean annual $\delta^{18}O$ difference (horizontal lines in Fig. 4) of these intervals is a relatively small 0.22‰. However, as noted previously, the overall reduction in winter and summer $\delta^{18}O$ from the peak of Medieval warming (~A.D. 975) to the extremes of LIA cooling (~A.D. 1720) is, respectively, 0.8 and 1.0‰. The summer temperature change, relative to the oceanic water vapor source temperatures (perhaps slightly lower at the height of the Little Ice Age), is 1.7°C when the regional 0.6‰/°C $\delta^{18}O$ gradient is applied. Bradley and Jones (1993) suggest a Northern Hemispheric summer temperature cooling of 0.9°C (relative to the summer temperatures of the 15th century) for the A.D. 1570–1730 interval. Greenlandic and Northern Hemispheric temperatures need not always be in phase, especially on a decadal scale, but the magnitude of change in both areas is comparable

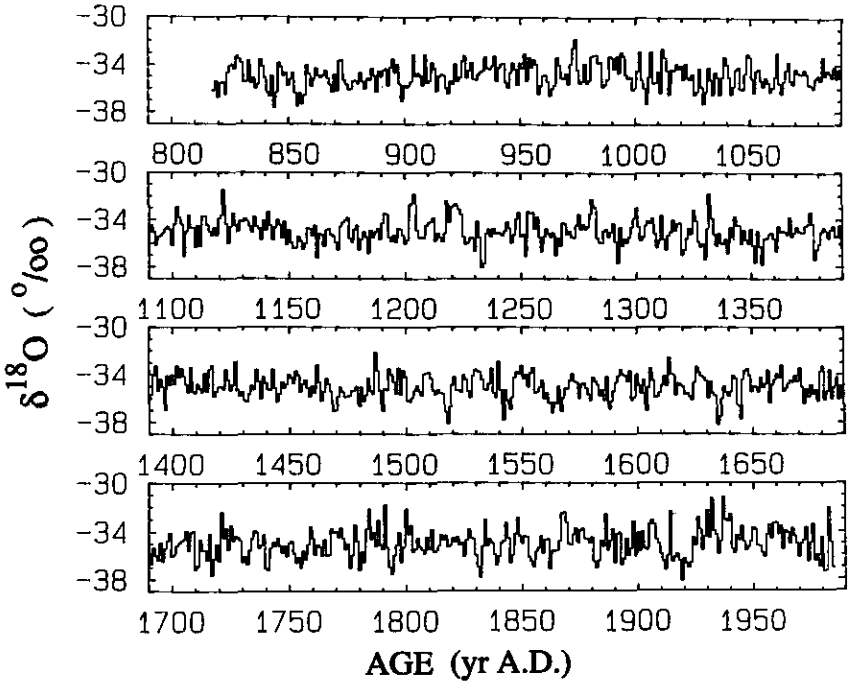

FIG. 2. Bar diagram of mean annual $\delta^{18}O$ values (‰), relative to Vienna SMOW, of GISP2 ice core samples. The 1167 year long cal yr B.P. record covers the A.D. 818–1985 interval (yr A.D. = 1950 − cal yr B.P.; 0 yr B.P. = A.D. 1950). Tickmarks are halfway between summer layers.

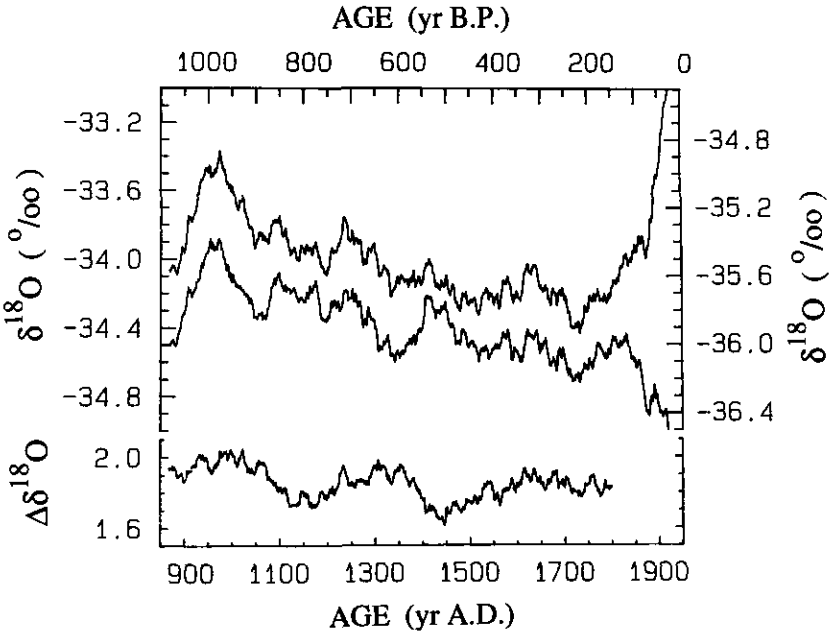

FIG. 3. One hundred year moving averages of highest (upper curve, left $\delta^{18}O$ scale) and lowest (middle curve, right $\delta^{18}O$ scale) $\delta^{18}O$ values (‰) encountered for each year. The bottom curve presents the $\delta^{18}O$ differences ($\Delta\delta^{18}O$) of the upper and middle curve and depicts summer–winter $\delta^{18}O$ contrast.

(as to be expected, the 1.7°C change at the GISP2 site (~73°N) exceeds the hemispheric mean).

One-hundred-year moving averages of annual accumulation (Meese *et al.,* 1994b) and annual $\delta^{18}O$ correlate with an r value of 0.19 for the current millennium ($r = 0.50$ for the MWP interval and 0.15 for the LIA interval). The above r values increase to 0.40, 0.51, and 0.46, respectively, when the moving averages of accumulation and summer–winter $\Delta\delta^{18}O$ are compared. The average percentage change in annual accumulation per ‰ $\delta^{18}O$, 3.1 ± 0.5% per ‰ for the A.D. 870–1800 interval, is less than the ~7.7% per ‰ for the larger late-glacial–Holocene trends in accumulation and $\delta^{18}O$ (Meese *et al.,* 1994b).

The early Viking settlements in Greenland (circa A.D. 985) date back to the MWP $\delta^{18}O$ maximum (~A.D. 975). The more-northern colony (also called Western Settlement) was abandoned about the mid-14th century (e.g., Lamb, 1977). Although our $\delta^{18}O$ fine structure (Fig. 4, bottom curve) is somewhat incomplete in that it probably does not register faithfully all winters, we note two very cold winters in A.D. 1352 and A.D. 1355 in the GISP2 $\delta^{18}O$ record (see also Fig. 2). Development of the A.D. 1351 and A.D. 1352 summers in the record also is very minimal and these summers were evidently very cold. The rapid succession of two disastrous growing seasons could have led to the abandonment of the Western Settlement. Our approximate dates are close to Ogilvie's (1984) recorded dates of severe Icelandic winters in A.D. 1350, 1351, and 1355.

The Eastern Settlement probably was deserted around the mid-15th century (Lamb, 1977). Here, abandonment would have been during the early stages of the Little Ice Age. We suggest, on the basis of the Figure 4 $\delta^{18}O$ fine structure, survival of the Eastern colony to at least A.D. 1468.

The long-term trends in the corrected GISP2 Holocene $\delta^{18}O$ record of 20-yr samples (Figs. 5 and 6) include climate amelioration in the early (Preboreal) part, a relatively stable optimal $\delta^{18}O$ level between about 10,000 and 2000 cal yr B.P. (a rather long Hypsithermal interval), with some interruptions (i.e., at 8200 cal yr B.P.) and a gradual decline from 2000 cal yr B.P. to the present.

Oceanic $\delta^{18}O$ reduction caused by the return of ice-cap waters contributes significantly to the relatively small 10,000–

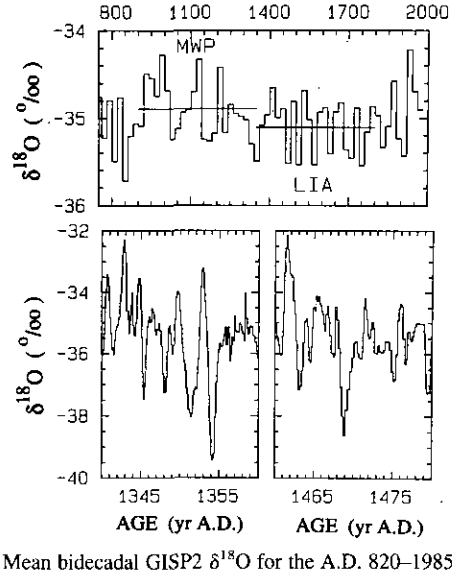

FIG. 4. Mean bidecadal GISP2 $\delta^{18}O$ for the A.D. 820–1985 interval (upper curve). The horizontal lines give average annual $\delta^{18}O$ for the Medieval Warm Period (MWP) and Little Ice Age (LIA). The lower curves provide intra-annual detail for the A.D. 1340–1360 and A.D. 1460–1480 intervals (tickmark year denotes the summer of that year).

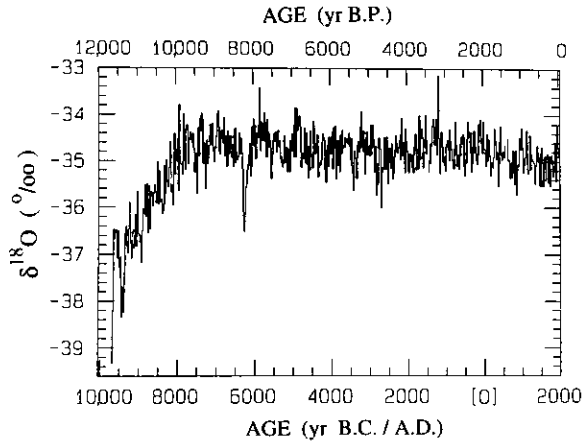

FIG. 5. Bar diagram (with 2 brief gaps) of Holocene $\delta^{18}O$ values (‰), relative to Vienna SMOW, of GISP2 ice core samples. Each bar spans 20 calibrated (cal) years. The termination of the Younger Dryas (at a depth of 1677 m) is at 11,640 ± 200 cal yr B.P. (Alley *et al.*, 1993; Meese *et al.*, 1994a).

5000 cal yr B.P. $\delta^{18}O$ change (we estimate the oceanic $\delta^{18}O$ enrichment at 10,000 cal yr B.P. relative to ~5000 cal yr B.P. at ~0.3‰). Of comparable importance is GISP2 Holocene ice sheet elevation change (up to 100m (Cuffey *et al.*, 1995; Cutler et al., 1995)).

ISOTOPIC AND VOLCANIC CONNECTIONS

Zielinski *et al.* (1994) have identified 43 volcanic eruptions ($SO_4^=$ residuals above 24 ppb) in the GISP2 core for the current millennium. Nearly all (83% over the last 2000 years) eruptions identified in the core can be matched with the historical (non-^{14}C dated) record, leading to the assignment of volcanic explosivity index (VEI) values (Newhall and Self, 1982) in the 3 to 7 range. As noted by Zielinski *et al.* (1994), the latitude of the volcano and the season in which the eruption occurred determines the time lag between eruption and deposition of (stratospheric) aerosols in Greenland. This lag can be up to 2 yr (even longer for equatorial eruptions, or eruptions occurring during the summer when there is less mixing between tropical and polar air masses).

We estimated the effect of volcanic (sulfurous) aerosols on climate by "stacking" annual $\delta^{18}O$ records. For each of the 43 volcanic eruptions identifiable in the GISP2 core for the current millennium, we took a slice of 15 yr of the $\delta^{18}O$ record. The GISP2 ice layer count was set to 0 for the year of eruption. Each interval extends from −7 to +7 yr. Stacking of intervals leads to mean $\delta^{18}O$ profiles (Fig. 7a) for the VEI 6-7 class (7 events), the VEI 4 group (20 events), and all eruptions (43 events). Initial climate cooling for the VEI 6-7 eruptions is noticed 3 yr ahead of the year of ice aerosol incorporation. There is a lead of 2 yr for the group of 43 events. The shorter lead relates to the influence of latitudinal distribution of the volcanic centers on aerosol transport times toward Greenland (the 43 events are more evenly spread over latitude than the mega events, 5 out of 7 being in equatorial regions). The $\delta^{18}O$ increase at +2 year for the mega eruptions most likely is related to baseline natural climate variability.

The 43 event $\delta^{18}O$ lowering lasts 4 to 5 yr. Maximum mean annual $\delta^{18}O$ reductions are 0.90 ± 0.42‰ (~1.5 ± 0.7°C), 0.75 ± 0.26‰ (~1.2 ± 0.44°C), and 0.45 ± 0.16‰ (~0.75 ± 0.27°C) for, respectively, the VEI 6-7 class, the VEI 4 group, and all volcanic events. Standard deviations were estimated from the scatter of "undisturbed" $\delta^{18}O$ of years −7 to −4 and +4 to +7.

Three individual eruptions are depicted in Figure 7b. "Natural" climate variability seems to obscure the Tambora $\delta^{18}O$ signal more than those of Krakatoa and Katmai and the "year without a summer" (A.D. 1816) is not very remarkable. The ice layer counts for the year of $SO_4^=$ detection in the ice core (our zero year) agree with the historical date for all 3 events. As the actual eruption must have taken place 2 to 3 years earlier, the ice layer count years (Meese *et al.*, 1994a) may need a correction of two years.

The central Greenland temperature depression will be maximal once the stratospheric aerosols have penetrated to Greenland latitudes. Ice aerosol incorporation occurs when strato-

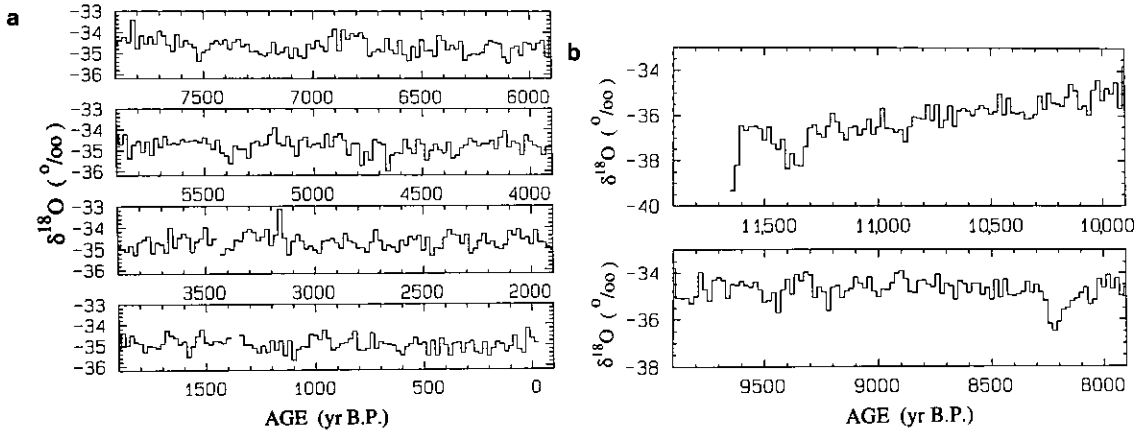

FIG. 6. Detailed subdivisions of the Fig. 5 $\delta^{18}O$ record.

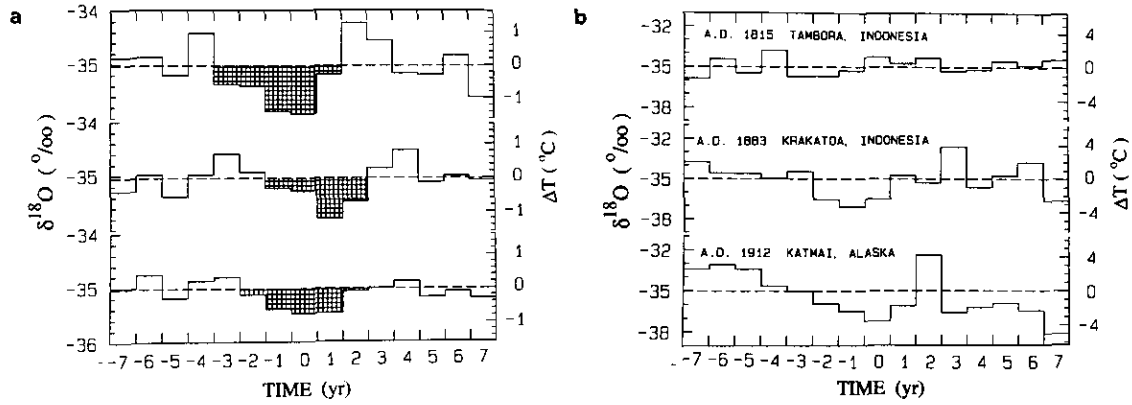

FIG. 7. (a) Mean stacked $\delta^{18}O$ values (see text) centered around the zero year in which volcanic emissions were detected in the GISP2 ice core for the current millennium (Zielinski *et al.,* 1994). Top curve, VEI 6 and 7 ($n = 7$); middle curve, VEI 4 ($n = 20$); and bottom curve, all detected emissions (of which 85% were identified as VEI 3 to 7; $n = 43$). The average $\delta^{18}O$ values of the "undisturbed" −7 to −4 and +4 to +7 yr (the averages are −35.02 and −35.03‰) yielded the dashed lines. $\delta^{18}O$ was converted to mean annual temperature using a 0.6‰/°C gradient. (b) $\delta^{18}O$ change during the historic A.D. 1815, 1883, and 1912 eruptions. Year zero is defined as in (a).

spheric aerosols mix down into the troposphere (primarily through the stratospheric-tropospheric gap in spring time at middle latitudes). Temperature depression in all Figure 7a averages is largest when aerosols are incorporated in the ice (yr 0). Following yr 0, the stratospheric aerosols are emptied rather rapidly and normal temperatures are reached by yr +2.

There are about 200 yr (out of ~1000) with mean annual temperature lowering of 0.5°C. Volcanic aerosols evidently reduced the mean temperature of our millennium at the GISP2 site by about 0.1°C.

ISOTOPIC AND SOLAR CONNECTIONS

Historical observations of the Sun's spottiness can be used for a comparison with ^{18}O data. The detailed sunspot record, however, extends only to the 17th century. Prior to the 17th century, $\Delta^{14}C$[2] and ^{10}Be have to substitute as proxies of solar change. These cosmogenic isotopes register solar change because the Sun (by way of the magnetic properties of the solar wind) influences the fraction of earth-bound galactic cosmic rays reaching the earth's atmosphere (Lingenfelter, 1963; O'Brien, 1979).

Fourier analysis of the 1168-yr single year $\delta^{18}O$ record (Fig. 2) yielded increased spectral power density (SPD) near 69, 29, 21, 19, 16, 11, 9, and 6.3–2.7 yr periodicities. The 11- and 21-yr periodicities may reflect solar influences on climate, given sufficient amplification of the small solar constant (E) changes related to the sunspot cycle (Schatten, 1988; Wilson and Hudson, 1988; van Loon and Labitzke, 1988). The 69-yr SPD increase falls within the 65–70 yr periodicity of a North Atlantic Ocean–Northern Hemispheric climate system oscillation (Schlesinger and Ramankutty, 1994). On the other end of the spectrum, the 2.7–6.3 yr periodicities correspond in duration to the irregular cycle of ENSO events (Quinn and Neal, 1992). A 18.6-yr cycle of air pressure, tied to lunar-solar tides (O'Brien and Currie, 1993), approximates the 19-yr periodicity.

SPD increases in Holocene bidecadal GISP2 $\delta^{18}O$ (Fig. 5) are near 3300, 1050, 550, 465, 314, 264, 242, 211, 155, and 120 yr. There are some similarities in ^{18}O and ^{14}C spectral periodicities (Stuiver and Braziunas, 1993) near 2500–3300, 830–1050, 520, 210, and 150 yr whereas SPD ^{18}O and ^{14}C peak matches are encountered for the annual records near 70, 61, and 46–44 yr. The 210 and 88 yr ^{14}C periodicities relate rather unequivocally to solar forcing (Stuiver and Braziunas, 1993; Damon and Sonett, 1991). The 88 yr ^{14}C periodicity has only a minor ^{18}O companion. A ~2500 yr periodicity was previously identified in the Camp Century ice core $\delta^{18}O$ profile (Dansgaard *et al.,* 1984).

Similarity of power spectra of $\delta^{18}O$ and $\Delta^{14}C$ may result from other common forcing factors such as oceanic thermohaline circulation (deep water formation) besides the Sun influencing climate ($\delta^{18}O$) and ^{14}C production rate simultaneously. Increased deep-water formation parallels increased northward heat transport in the North Atlantic (Stuiver and Braziunas, 1993; Broecker and Denton, 1989). This scenario predicts higher GISP2 $\delta^{18}O$ (warmer climate in the North Atlantic region) when atmospheric (global) $\Delta^{14}C$ is lower. Little is known about the extent to which climate is influenced by thermohaline circulation change.

For solar forcing, estimations of related $\delta^{18}O$ change are possible. Sunspot number change (determinable from the $\Delta^{14}C$ record) is tied to solar "constant" change, and solar constant change induces a climatic ($\delta^{18}O$) response of which the magnitude can be estimated from climate models. Predicted $\delta^{18}O$ and ^{14}C production rates (Q) (calculated from the $\Delta^{14}C$ profile; Braziunas, 1990) have opposite phases for solar forcing, similar to that of thermohaline forcing. Our calculations (Stuiver and Braziunas, 1993; Stuiver and Quay, 1980) show that a 1%

[2] $\Delta^{14}C$ (‰) is the relative deviation of the measured ^{14}C activity from the U.S. National Bureau of Standards (NBS) oxalic acid standard activity, after correction for isotope fractionation and decay related to age (Stuiver and Polach, 1977). High-precision treering $\Delta^{14}C$ reproducibility is 1.5 to 3‰.

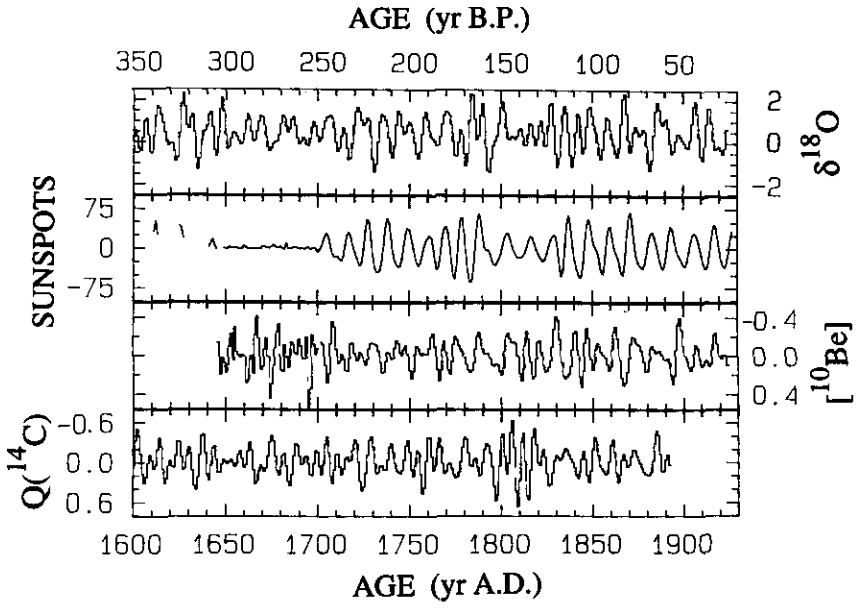

FIG. 8. Filtered (filter range 5–20 yr) GISP2 ice core $\delta^{18}O$, sunspot numbers, ice core ^{10}Be concentration (Beer *et al.*, 1990, 1994), and ^{14}C production rates (Q) for the A.D. 1600–1930 interval. The ^{10}Be and Q scales are inverted. Units: $\delta^{18}O$, in ‰; sunspots, actual numbers; ^{10}Be and Q, as fractional deviations from the means.

increase in ^{14}C production rate Q ultimately predicts a climatic $\delta^{18}O$ lowering of about 0.018‰ (this is an upper limit, as the $\delta^{18}O$ change will be smaller to the extent that the ocean source waters cool).

For the (postulated) solar cycles near 61, 88, 210, and 530 yr, predicted (from $\Delta^{14}C$) and observed $\delta^{18}O$ average peak to trough swings (of filtered records) are, respectively, 0.16‰ (~0.27°C) and 0.25‰ (~0.42°C). The absolute magnitude of the "cycles" is small relative to the 0.140‰ σ of a single $\delta^{18}O$ measurement and the differences also are not significant, given the inherent uncertainties of the basic tenets (such as linearity between sunspot number and solar constant, and the neglect of amplification (if any) of the solar signal in our complex atmosphere). Evidently solar modulation could be responsible for the fairly small temperature (~0.4°C) variations associated with these cycles. Absolute proof of a correlation, however, is lacking because correlation coefficients between filtered $\delta^{18}O$ and $\Delta^{14}C$ (corrected for the Q–$\Delta^{14}C$ phase lag) for the four cycles are small (r values −0.07 to +0.23) due to time-variable phase relationships.

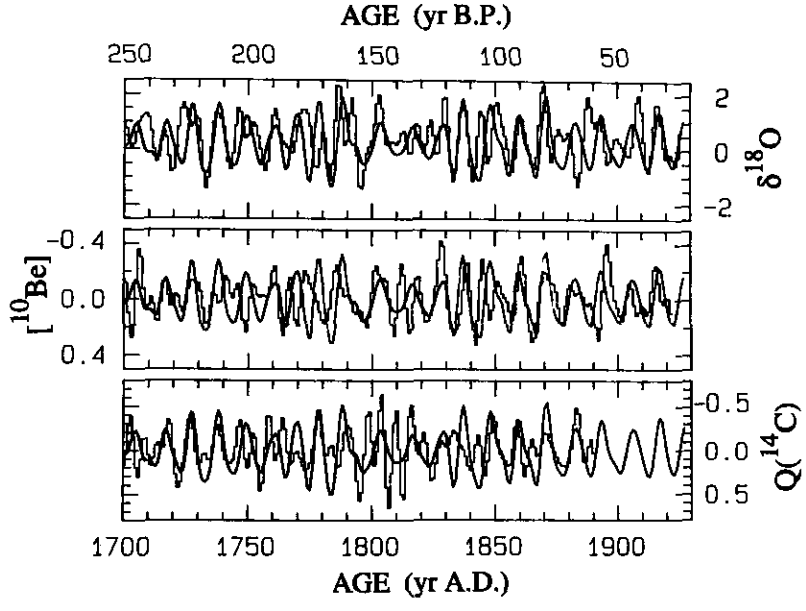

FIG. 9. Similar to the A.D. 1700–1930 interval in Fig. 8, but with a 2-yr shift for $\delta^{18}O$ toward the past and 2-yr advancements for ^{10}Be and $Q(^{14}C)$ (see text). Heavy solid line is the filtered sunspot number curve.

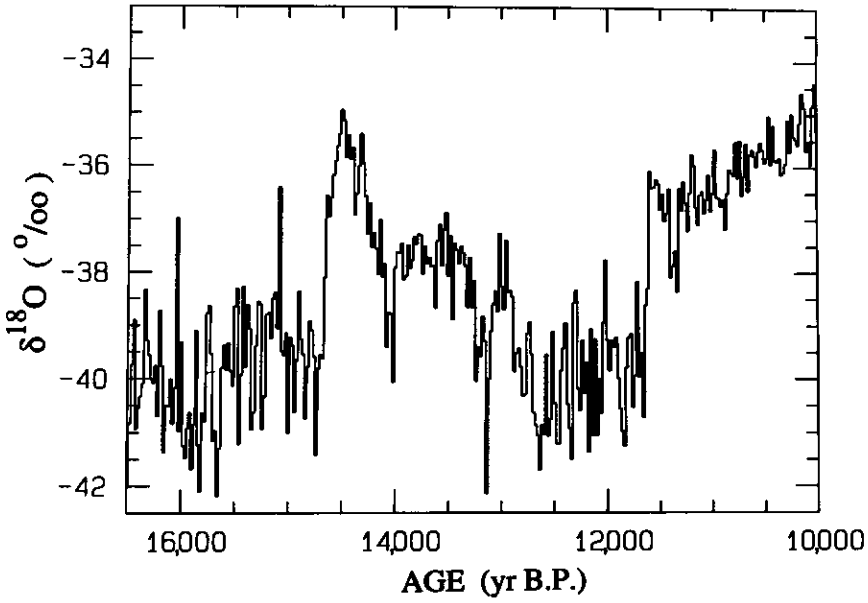

FIG. 10. GISP2 bidecadal $\delta^{18}O$ for the interval 16,500–10,000 cal yr B.P.

Given uncertainties in spectral analysis, and some overlap in the 830 yr $\Delta^{14}C$ and 1050 yr $\delta^{18}O$ spectra, one cannot immediately reject the notion of a possible tie between $\Delta^{14}C$ and $\delta^{18}O$ in the 1000 yr range. In fact, the filtered (750–1100 yr filter) $\Delta^{14}C$ (corrected for the Q–$\Delta^{14}C$ phase lag) and $\delta^{18}O$ records yield an r value of –0.73. The substantial difference in calculated and observed $\delta^{18}O$ (respectively, 0.12‰ (~0.20°C) and 0.35‰ (~0.70°C), peak to trough) is suggestive of a non-solar source, such as thermohaline circulation change.

For the ~2500 year cycle, predicted and observed $\delta^{18}O$ are of similar magnitude. Without lagging the records, the r value is +0.76. Positive r values, however, do not conform with solar or thermohaline forcing. Another (as yet unidentified) mechanism may play a role.

GISP2 $\delta^{18}O$ as well as annual $\Delta^{14}C$ (A.D. 1510–1954 interval; Stuiver and Braziunas, 1993) display increased spectral power density for periodicities in the 10 to 11 yr range. Application of a 5–20 yr filter to sunspot numbers (S) (Eddy, 1976), annual ice core $\delta^{18}O$, ^{10}Be in the Dye 3 core (Beer *et al.*, 1990, 1994), and calculated ^{14}C production rate Q (using annual atmospheric $\Delta^{14}C$) yielded the $\delta^{18}O$, ^{10}Be, Q, and S records of Figure 8. There are noticeable similarities, e.g., the simultaneous reduction in $\delta^{18}O$ and S variance during the Maunder (late 17th century) and Dalton (early 19th century)

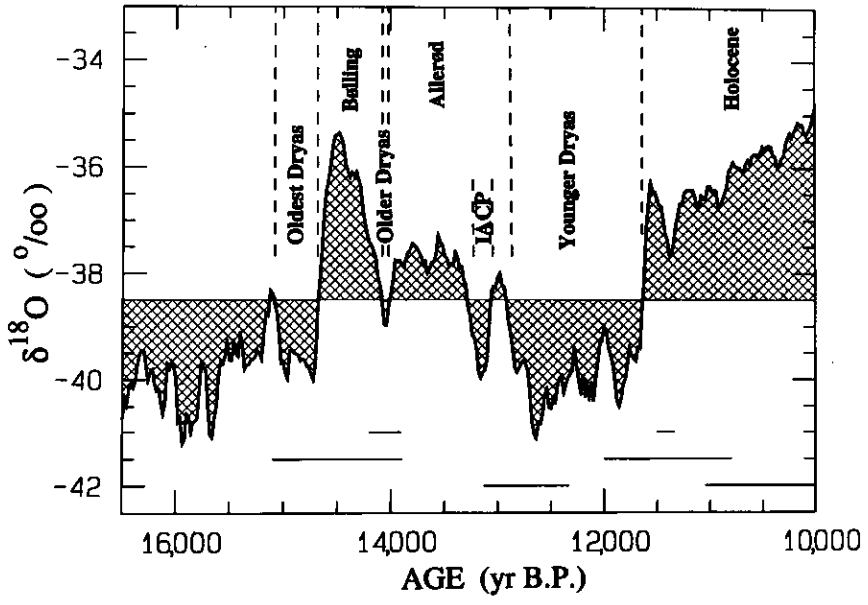

FIG. 11. Major $\delta^{18}O$ climate transitions (solid line is a five-point (100-yr) moving average of Figure 10 $\delta^{18}O$ values) and European pollen zone boundaries (see text). Horizontal lines denote suggested periods of rapid sealevel rise (top, Blanchon and Shaw, 1995; middle and bottom, estimated, respectively, from Fairbanks *et al.*, 1992 and Edwards *et al.*, 1993).

TABLE 2
Ages of Stratigraphic Boundaries

Chronostratigraphy	^{14}C age (yr B.P.)	Ice layer count (cal yr B.P.)
Holocene		
Younger Dryas	10,000[a]	11,650
Allerød	11,021 ± 25[b]	12,890
Intra-Allerød cold period (IACP)		13,070
Allerød	11,730 ± 100[c]	13,250
Older Dryas	11,800[a]	14,010
Bølling	12,000[a]	14,090
Oldest Dryas	~12,500[d]	14,670
		~15,070

[a] Mangerud *et al.* (1974).
[b] Björk and Möller (1987).
[c] Lehman and Keigwin (1992). This marine date (reservoir corrected by 440 ^{14}C yr) was not plotted in Figure 12 because the ^{14}C reservoir deficiency correction is uncertain (see also Bard *et al.*, 1994).
[d] Nilsson (1983).

minima in sunspot numbers. In Figure 9 we compare filtered isotopic cycles directly with the filtered sunspot cycle for the A.D. 1700–1930 interval. Again the synchronous reduction of $\delta^{18}O$ (step curve) and sunspot number S (smooth curve) variability during the early 19th century is impressive (S increase implies solar constant increase).

When correlating $\delta^{18}O$, $\Delta^{14}C$, Q, and ^{10}Be relative to S, the highest correlation coefficient is encountered for $\delta^{18}O$ leading S by 2 yr. Similarly, for optimal correlation, both Q and ^{10}Be lag S by 2 yr. The lead/lag numbers have an uncertainty that is difficult to estimate, and the rather surprising $\delta^{18}O$ lead disappears if ice layer counts are systematically in error by 2 yr, as suggested by our volcanic discussion (an additional 0.5-yr correction is tied to the use of summer–summer ice layer count years). The observed ^{10}Be concentration lag, however, agrees with a ^{10}Be tropospheric + stratospheric residence time of about 2 yr. Our model carbon reservoir lacks a stratosphere–troposphere barrier so that calculated Q (starting from observed $\Delta^{14}C$) will lag actual Q by about 2 yr. As the lag between actual Q and S is only a fraction of a year, the observed 2-yr lag between calculated Q and S is fully compatible with Q forcing by the Sun of the 11-yr $\Delta^{14}C$ cycle.

In Figure 9 the $\delta^{18}O$ curve was advanced, and the ^{10}Be and Q curves lagged, by 2 yr. S, as expected, is in phase with $\delta^{18}O$. Because S is in antiphase with cosmogenic isotope production, we inverted the ^{10}Be and $Q(^{14}C)$ scales in Figures 8 and 9.

Taking autocorrelation into account, the probability that a significant correlation ($r = +0.36$) between $\delta^{18}O$ and S is lacking is less than 0.4% for the A.D. 1700–1924 interval (filtering removes the "ends" of the record). The r values for the A.D. 1702–1924 ^{10}Be-S and A.D. 1700–1892 $Q(^{14}C)$–S comparisons (with 2-yr lags applied) are, respectively, −0.29 and −0.34, implying significance levels of 0.5 and 0.2%. The correlation coefficients are negative, in agreement with 20th century observations of S and cosmic-ray-induced atmospheric neutron flux (see Beer *et al.*, 1990, 1994, for detailed ^{10}Be discussions).

Our analysis connects 11-yr climate and solar variability. Such a connection has been suggested previously (e.g., Labitzke and Van Loon, 1988). In fact, the other cyclic temperature changes are dwarfed by the ~2.6°C changes ($\delta^{18}O$ change of 1.55‰, peak to trough) of the "11 year" cycle of annual $\delta^{18}O$ (5–20 yr filter). However, the forcing mechanism remains obscure, as the physical mechanism for a substantial amplification of the small change in solar constant (Wilson and Hudson, 1988) has not been identified. The predicted $\delta^{18}O$ change

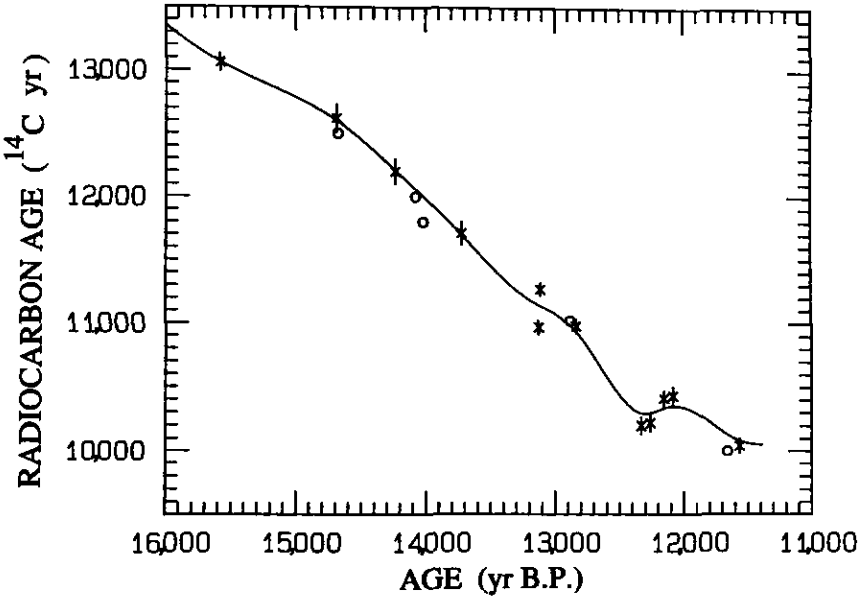

FIG. 12. Reservoir corrected coral radiocarbon ages (crosses) versus U/Th age (Bard *et al.*, 1993, Edwards *et al.*, 1993). Vertical bar denotes standard deviation. Circles are radiocarbon dates (see text) of major climate transitions found in the $\delta^{18}O$ record (Fig. 11). The spline (solid line) is based on coral data only.

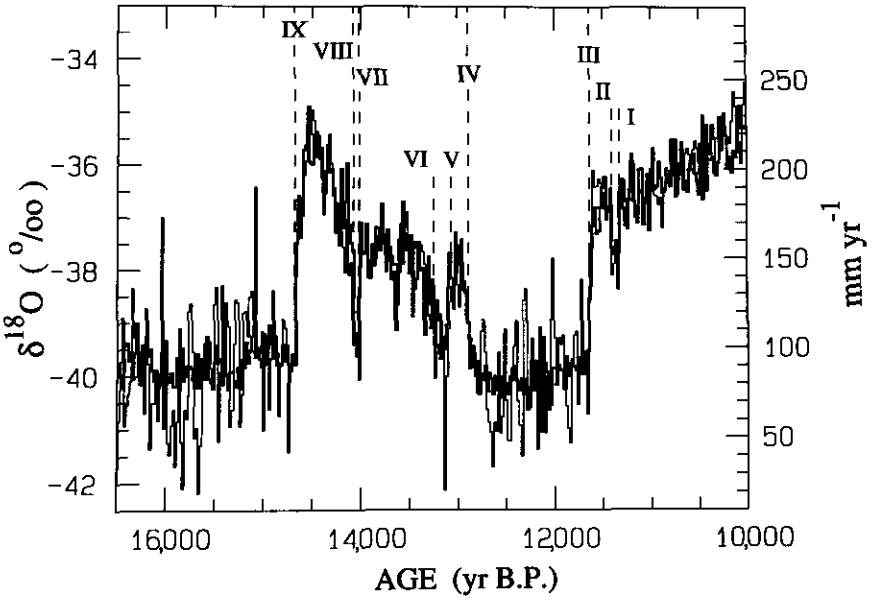

FIG. 13. Annual accumulation rate (heavy solid line, Alley *et al.*, 1993, Meese *et al.*, 1994b) and $\delta^{18}O$ (light line), both averaged over 20-yr intervals. The fast climate transitions (labeled with Roman numbers) are detailed in Fig. 14.

is only ~0.54‰ (peak to trough). Other factors, such as oscillatory behavior on a decadal scale of the earth's atmosphere–ocean system and $\delta^{18}O$ depression by volcanic aerosols (the historical record of large volcanic eruptions contains an 11-yr component; Stothers, 1989) must have contributed to the $\delta^{18}O$ variability (1.55‰) in this frequency band.

$\delta^{18}O$ CLIMATE TRANSITIONS AND ^{14}C AGE CALIBRATION 16,500–10,000 CAL YR B.P.

The bidecadal GISP2 $\delta^{18}O$ results for the 16,500–10,000 cal yr B.P. interval are depicted in Figure 10. A correlation with GRIP data (Dansgaard *et al.*, 1993) yielded an r value of 0.93 for this interval. It contains the classical Oldest Dryas (OD1)–Bølling (B)–Older Dryas (OD2)–Allerød (A)–Younger Dryas (YD)–Holocene sequence (Nilsson, 1983; Johnson *et al.*, 1992) as labeled in Figure 11. There is an intra-Allerød cold period (IACP) manifested in Norwegian Sea *N. pachyderma* frequency distributions (Lehman and Keigwin, 1992).

Figure 11 represents a 5-point (100 yr) moving average of the Figure 10 bidecadal points. The OD1–B–OD2–A–YD and IACP climate boundaries in Figure 11 are matched with major shifts in $\delta^{18}O$. We used the intercepts of the Figure 10 climate transitions with the $\delta^{18}O = -38.5$‰ "baseline" to fix the ice layer count years in Table 2.

Independently determined ^{14}C ages for the Figure 11 climate transitions can be tied to ice layer count years (Table 2). The standard deviations in the radiocarbon ages of the transitions are not always well defined, but range from 25 ^{14}C yr to an estimated 150 ^{14}C yr. In Figure 12 we compare the ^{14}C–cal age (ice layer count) relationship with that obtained from ^{14}C and U/Th dating of corals (Bard *et al.*, 1993; Edwards *et al.*, 1993; Stuiver and Reimer, 1993) and find excellent agreement.

The coral ^{14}C ages were lowered by 400 yr, the average ^{14}C reservoir ages of the current world surface ocean waters. Paleodeviations are possible (Bard *et al.*, 1994). If our global thermohaline circulation were reduced during the 16,000–12,000 cal yr B.P. interval (see below), surface ^{14}C reservoir ages in coral habitat regions would be less, but only by a limited amount (~50 yr; Stuiver *et al.*, 1995).

Table 2 equates GISP2 cal ages of $\delta^{18}O$ changes in Greenland ice to radiocarbon ages of major pollen zone boundaries in Europe. A zero time lag between the major Greenlandic and European climate events is implied. This assumption is based on the notion that northwestern Europe, Greenland, and the North Atlantic have substantial climatic interdependence.

Not all suggested intervals of increased sea-level rise (Fairbanks *et al.*, 1992; Edwards *et al.*, 1993; Blanchon and Shaw, 1995) appear to be firmly anchored to major climate warming (Fig. 11, horizontal bars). The Blanchon and Shaw terminations of sea-level rises, however, are synchronous with the cooling episodes of the Older Dryas and of the Holocene event near 11,300 cal yr B.P.

The causes of the Younger Dryas event are widely researched. An equally important puzzle is the failure of the strong Bølling warming pulse to produce an "Early Holocene." The Oldest Dryas $\delta^{18}O$ baseline is about –39.5‰ whereas the Younger Dryas one is about –40‰. The Bølling oscillation, most of which is initiated in a mere 10 yr (with a $\delta^{18}O$ increase of 3‰), reaches a maximum at –35‰ after about 180 yr. The Younger Dryas–Holocene change starts almost equally fast, with $\delta^{18}O$ increasing by about 4‰ in 20 yr. Subsequent Holocene $\delta^{18}O$ change (contemporaneously with the breakup and melting of the Laurentide and Fennoscandian ice sheets) is slow, and the –35‰ level is only reached after about 1200 yr.

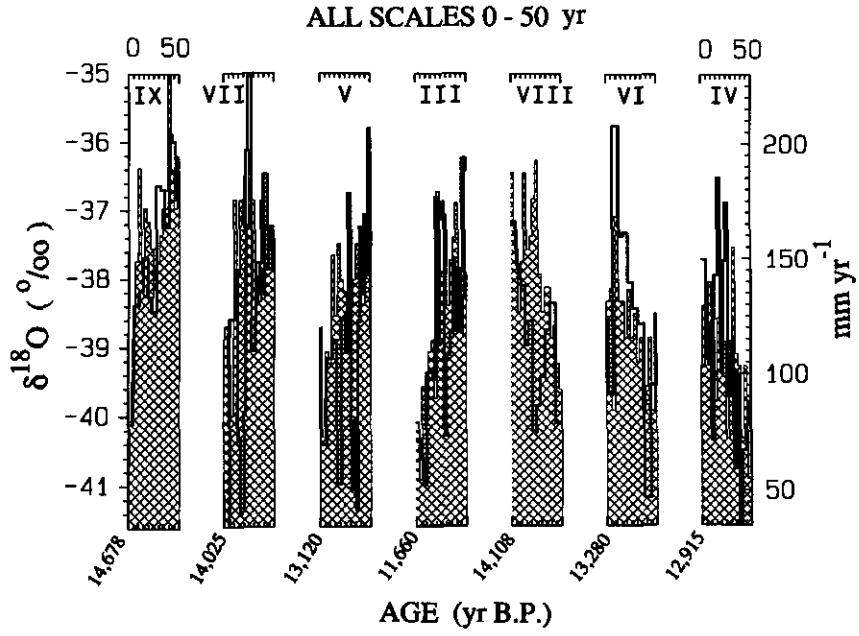

FIG. 14. Rapid $\delta^{18}O$ and accumulation rate transitions in the climate system. Heavy line depicts $\delta^{18}O$, light line and shaded area represents accumulation rate (Alley *et al.*, 1993, Meese *et al.*, 1994b). Transitions with Roman numerals are identified in Fig. 13. Horizontal bars represent 3 yr for the accumulation rates and range from 3 to 10 yr for the $\delta^{18}O$ data.

$\delta^{18}O$, ATMOSPHERIC CIRCULATION PATTERNS, AND SNOW ACCUMULATION RATES

There is a substantial increase in high-frequency (bidecadal) $\delta^{18}O$ variance (Fig. 10) during the cold intervals of the last glacial maximum (16,500–14,700 cal yr B.P. portion) and the Younger Dryas interval (12,400–11,700 cal yr B.P. portion). The σ of the bidecadal residual $\delta^{18}O$ values around the 100-yr trend (5-point moving average) is, respectively, 0.88 and 0.82‰ for the above intervals (''atmospheric circulation mode A''). The warmer (''atmospheric circulation mode B'') Bølling–Allerød (14,500–12,900 cal yr B.P. portion, exempting the OD and IACP intervals) and early Holocene (11,600–10,000 cal yr B.P. portion) exhibit much lower bidecadal σ's (respectively, 0.41 and 0.39‰).

One explanation for mode A doubling of bidecadal $\delta^{18}O$ variance is tied to shifts in atmospheric circulation (e.g., Kapsner *et al.*, 1995). During glacial episodes, a jet stream may split in two branches over North America, with the southern branch shifted far south over the Atlantic (Kutzbach and Webb, 1993). The northern branch would advect moisture from the North Pacific and travel a much colder path before reaching Greenland. An alternative scenario would be moisture advection, mostly from the Atlantic, with significant time-dependent differences in jetstream pathways.

Model experiments (Charles *et al.*, 1994) suggest that Greenlandic $\delta^{18}O$ of a North Pacific source would be as much as 15‰ below that of an Atlantic counterpart. Assuming a North Pacific source, the observed flip-flops in bidecadal mode A $\delta^{18}O$ (maximally ~4‰, from ~–42 to ~–38‰) could be generated by abrupt changes in the ratio of moisture transport of the Northern versus Southern jet stream branches, without necessarily generating major changes in mean annual temperature or accumulation rate at the Greenland site. The bidecadal $\delta^{18}O$ shifts during climate mode A would then be compatible with an upper limit shift in moisture transport of about one quarter of the joint total (given a 15‰ difference in $\delta^{18}O$ of precipitation supplied by the two branches).

A one-quarter magnitude change in moisture transport between branches does agree with the changes in ice core dust concentration between 16,500 and 14,700 cal yr B.P. High-resolution calcium records (Mayewski *et al.*, 1994) exhibit substantial bidecadal variability during this interval. Bidecadal residual Ca and $\delta^{18}O$ correlate with an r value of –0.42 (probability of no correlation is <0.1%). Higher dust content corresponds with lower $\delta^{18}O$, pointing toward increased transport of (Chinese?) dust when moisture transport shifts towards the northern jet stream branch. There is a change in residual ppb Ca of $-7.2 \pm 1.6\%$ per ‰ $\delta^{18}O$, indicating a ~29% switch in dust transport for the larger (4‰) bidecadal $\delta^{18}O$ swings.

Younger Dryas bidecadal $\delta^{18}O$ residuals and their Ca counterparts correlate with an r value of –0.05 only. Subtle climate differences may have disconnected the residual bidecadal Ca–$\delta^{18}O$ relationship found for the earlier interval (the Ca levels of the Younger Dryas do not quite reach the earlier late-glacial levels when sealevel was ~40 m higher (coastal plains) and ice sheet thickness was less).

Of the Figure 10 climate transitions, the most rapid are the initiations of the Bølling and Holocene, with $\delta^{18}O$ rates of change (β) of ~0.25‰/yr. The average β of four pre-Holocene warming transitions is ~0.14‰/yr whereas the corresponding average β for three downward trends is ~–0.07‰/yr. The $\delta^{18}O$

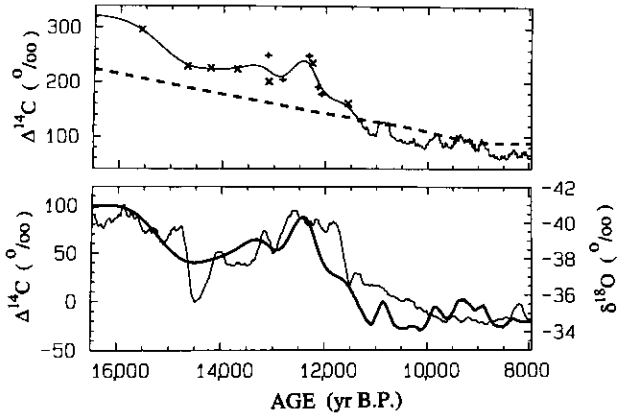

FIG. 15. (upper) $\Delta^{14}C$ values calculated from (1) geomagnetic dipole intensity change (dashed line) and (2) tree-rings (back to about 11,400 cal yr B.P.) and corals (crosses Bard *et al.*, 1993, plusses Edwards *et al.*, 1993). The upper window spline is the $\Delta^{14}C$ equivalent of the Fig. 12 spline. (lower) Light solid line is a 200-yr moving average of the Fig. 10 $\delta^{18}O$ values (inverted scale). Heavy solid line gives "geomagnetically free" residual $\Delta^{14}C$ (smoothed by taking a 200-yr moving average for the tree-ring $\Delta^{14}C$ values). See text.

inertia in the climate system evidently is such that downward shifts take longer than warming transitions. The much smaller Holocene variation at ~11,300 cal yr B.P. has reversed gradients (β's of ~−0.14‰/yr versus ~0.06‰/yr).

Isotopic smoothing of $\delta^{18}O$ step boundaries has occurred. Molecular diffusion in solid ice will progress over a distance of about 2 to 3 cm (Johnson and Robin, 1983) on each side of a step boundary in ~12,000 yr. Layer thickness is about 2.5 cm (~1 yr) in this part of the GISP2 core and diffusion would tilt a 3‰ $\delta^{18}O$ step change in Figure 14 by only half a degree. Vapor diffusion in the firn also adds to isotopic smoothing prior to polar ice inclusion. Because total diffusion length of water molecules in the firn is limited to a fraction (about 8 cm ice equivalent, Johnson and Robin, 1983) of an annual layer (~25 cm), this effect again is relatively minor.

There is substantial similarity in patterns of annual snow accumulation rate (α) and $\delta^{18}O$ for long-term (millennia) climatic changes (Alley *et al.*, 1993; Meese *et al.*, 1994b; Kapsner *et al.*, 1995). Similar to $\delta^{18}O$, the accumulation record points toward very fast climate transitions at the start of the Bølling and the Holocene (Alley *et al.*, 1993). In Figure 13 we compare the bidecadal $\delta^{18}O$ record to that of bidecadal annual accumulation (correlation coefficient $r = 0.90$). There is no demonstrable lag between $\delta^{18}O$ and α for most of the rapid transitions (Fig. 14, with a higher resolution of 3 yr for accumulation rate and 3 to 10 yr for $\delta^{18}O$).

The high residual bidecadal $\sigma^{18}O$ of 0.85‰ for atmospheric circulation mode A (cold) accompanies a residual bidecadal annual accumulation σ_α of 6.6 mm, a $\sigma_\alpha/\bar{\alpha}$ value of 7.5%, and a $\sigma_\alpha/\bar{\alpha}$ to $\sigma^{18}O$ ratio (γ) of 8.8% per ‰. For mode B (the warmer episodes) bidecadal $\sigma^{18}O = 0.40$‰, bidecadal $\sigma_\alpha = 10.3$ mm, $\sigma_\alpha/\bar{\alpha} = 5.9\%$, and γ equals 14.8% per ‰. With similar levels of bidecadal percent annual accumulation variability (Alley *et al.*, 1995), the differences in γ reflect mainly the increased mode A $\delta^{18}O$ variance (unconnected with accumulation rate changes) associated with switching between jet stream trajectories.

Long-term trends in $\delta^{18}O$ and percent accumulation rate track each other faithfully for mode B Bølling–Allerød and Preboreal episodes, with r values respectively, of 0.83 and 0.72, and an $\alpha/\bar{\alpha}$% versus $\delta^{18}O$‰ gradient (q) of 13.7 ± 1.1 and 9.5 ± 1.0% per ‰. For mode A we find a much lower q value of 1.7 ± 1.1% per ‰ ($r = 0.18$; Kapsner *et al.*, 1995). The correlation coefficients between bidecadal residual (100-yr trend removed) $\delta^{18}O$ and $\alpha/\bar{\alpha}$% are a minimal 0.05 for mode A, but increase to 0.15 and 0.39 (the Bølling-Allerød and Preboreal intervals) for mode B.

Although a Greenlandic $\delta^{18}O$–temperature (T) relationship is reasonably well established for our current climate system, the analogue gradient for mode A and B atmospheric circulation can only be estimated. The oscillatory $\delta^{18}O$ behavior of mode A points toward a relatively unstable (branched) circulation system where $\delta^{18}O$ variability is substantially increased relative to $\alpha/\bar{\alpha}$% change, and probably also T, suggesting a $\delta^{18}O$–T coefficient different than the current 0.6‰/°C. Whatever triggered mode B warming, the change must have immediately influenced the delicately balanced system of mode A. In fact mode B, which resembles a more southern version of our present atmospheric circulation system, obliterated mode A almost instantaneously (within a few years; Fig. 14).

The 5‰ $\delta^{18}O$ mode B initiations for the start of the Bølling and the Holocene (Fig. 10) represent substantial temperature change. Borehole temperatures (Gundestrup *et al.*, 1993; Cuffey *et al.*, 1995) indicate a mean glacial history 12°C colder than the present which leads to a $\delta^{18}O$–T gradient of ~0.4‰/°C for mode B initiations.

Thermodynamic factors and storm track changes both play a role in regulating percent annual accumulation change per °C. Here we assume dominance of thermodynamic control for the major climatic episodes. Such control implies an accumulation rate increase of 4% per °C, or slightly more (Kapsner *et al.*, 1995). Applying the 4% per °C coefficient to the above q values leads to $\delta^{18}O$–T gradients of 0.28 ± 0.02, 0.42 ± 0.04, and 2.4 ± 1.6‰/°C, respectively, for the Bølling–Allerød and the Preboreal mode B episodes, and the glacial mode A intervals. The mode B gradients derived in this manner are similar in magnitude to the borehole-derived ~0.4‰/°C value, and the mode A gradient increase (albeit with a large uncertainty) agrees with our interpretation of a branched jet stream system.

The above $\delta^{18}O$–T gradient switches are compatible with storm track changes occurring during (1) the nearly instantaneous switch from mode A to B and (2) the northward shift of the mode B circulation system during progressive stages of deglaciation. Acceptance of the above gradients for the interpretation of GISP2 $\delta^{18}O$ indicates reduced T variance during mode A episodes, and a T enhancement for the Bølling transition relative to the Younger Dryas–Holocene one.

LONG-TERM ISOTOPIC AND OCEANIC CONNECTIONS

Atmospheric ^{14}C levels depend on the relative isotope distribution between the earth's various carbon reservoirs. The current deep ocean and thermocline contain about 90% of the globally exchangeable ^{14}C. The amount of ^{14}C in the deep ocean (and indirectly the atmosphere) depends on the rate of ^{14}C transfer through deep water formation. For a full cessation of ^{14}C transfer toward the deep ocean, the available cosmic-ray-produced ^{14}C would be distributed over a 10 times smaller global carbon reservoir, causing a 10-fold increase in atmospheric ^{14}C concentration.

In this section we explore the tie between climate ($\delta^{18}O$) and oceanic thermohaline circulation change ($\Delta^{14}C$) for the late-glacial to early Holocene interval. Increased deep water formation (and the accompanying increase in upwelling of older ^{14}C-deficient Atlantic waters) will lower atmospheric $\Delta^{14}C$ while the concomitant increase in the flux of northward-flowing surface water increases heat transport in the North Atlantic and ice core $\delta^{18}O$.

We removed geomagnetic dipole intensity change as a forcing factor (e.g., Mazaud *et al.,* 1991) by deducting its model-calculated $\Delta^{14}C$ contribution (Stuiver *et al.,* 1991) using the McElhinny and Senanayake (1982) data set of paleomagnetism. In Figure 15 (upper window) we present atmospheric $\Delta^{14}C$ values (as derived from a spline through the radiocarbon ages of U/Th dated corals (Bard *et al.,* 1993; Edwards *et al.,* 1993)) and our model-calculated geomagnetic $\Delta^{14}C$ profile. The lower window compares residual atmospheric $\Delta^{14}C$ (obtained by deducting the geomagnetic contribution) to the inverted GISP2 $\delta^{18}O$ (200-yr moving average) profile. The correlation coefficient, r, indeed is negative (warmer climate coexisting with lower residual atmospheric $\Delta^{14}C$) and the residual $\Delta^{14}C$–GISP2 $\delta^{18}O$ correlation coefficient is a healthy –0.84 for the interval 16,500–10,000 cal yr B.P.

There is a suggestion that North Atlantic oceanic thermohaline circulation increase leads central Greenland climate ($\delta^{18}O$) by about 400 yr. As noted previously (Stuiver and Braziunas, 1993), the onset of increased thermohaline circulation leading to the Holocene would have been early in Younger Dryas time near 12,400 cal yr B.P. The ^{14}C pattern shows overall thermohaline circulation to be of similar magnitude when approaching the Bølling and the Holocene. The circulation increase during the Bølling, however, is substantially below that of the Holocene.

ACKNOWLEDGMENTS

We acknowledge the funding of the $\delta^{18}O$ (Grant OPP-9321164) and $\Delta^{14}C$ (Grant ATM-9310121) research of the Quaternary Isotope Laboratory by the National Science Foundation. We thank the PICO drillers, the Science Management Office (University of New Hampshire), and the Polar Ice Coring Office (Alaska) for logistics support, and GISP2 colleagues (i.e., R. B. Alley, P. M. Mayewski, D. A. Meese, and M. S. Twickler) and J. Beer for their sharing of data and field assistance. The field work of T. Saling, the ^{18}O and ^{14}C expertise of P. J. Wilkinson and P. J. Reimer, and comments from R. B. Alley, P. E. Damon, and S. J. Lehman are much appreciated.

REFERENCES

Alley, R. B., Meese, D. A., Shuman, C. A., Gow, A. J., Taylor, K. C., Grootes, P. M., White, J. W. C., Ram, M., Waddington, E. D., Mayewski, P. A., and Zielinski, G. A. (1993). Abrupt increase in Greenland snow accumulation at the end of the Younger Dryas event. *Nature* **362,** 527–529.

Alley, R. B., Spinelli, G. A., Zielinski, G. A., Taylor, K. C., and Shuman, C. A. (1995). Time-evolution of climate variability in Central Greenland from the GISP2 deep ice core, and the 8.2 ka event: Instability in the absence of large, mid-latitude ice sheets. [abstract] *EOS* **76**(17), S716.

Bard, E., Arnold, M., Fairbanks, R. G., and Hamelin, B. (1993). ^{230}Th-^{234}U and ^{14}C ages obtained by mass spectrometry on corals. *Radiocarbon* **35,** 191–199.

Bard, E., Arnold, M., Mangerud, J., Paterne, M., Labeyrie, L., Duprat, J., Mélières, M-A., Sønstegaard, E., and Duplessy, J-C. (1994). The North-Atlantic atmosphere–sea surface ^{14}C gradient during the Younger Dryas climatic event. *Earth and Planetary Science Letters* **126,** 275–287.

Barlow, L. K. (1994). Evaluation of seasonal to decadal scale deuterium and deuterium excess signals, GISP2 ice core, Summit, Greenland, A.D. 1270–1985. Ph.D. dissertation, Univ. of Colorado.

Beer, J., Blinov, A., Bonani, G., Finkel, R. C., Hofmann, H. J., Lehmann, B., Oeschger, H., Sigg, A., Schwander, J., Staffelbach, T., Stauffer, B., Suter, M., and Wölfli, W. (1990). Use of ^{10}Be in polar ice to trace the 11-year cycle of solar activity. *Nature* **347,** 164–166.

Beer, J., Joos, F., Lukasczyk, Ch., Mende, W., Rodriguez, J., Siegenthaler, U., and Stellmacher, R. (1994). ^{10}Be as an indicator of solar variability and climate. *In* "The Solar Engine and Its Influence on Terrestrial Atmosphere and Climate" (E. Nesme-Ribes, Ed.), *NATO ASI series I: Global Environmental Change*, Vol. 25, pp. 221–233. Springer-Verlag, Heidelberg.

Björck, S., and Möller, P. (1987). Late Weichselian environmental history in southeastern Sweden during the deglaciation of the Scandinavian Ice Sheet. *Quaternary Research* **28,** 1–37.

Blanchon, P., and Shaw, J. (1995). Reef drowning during the last deglaciation: Evidence for catastrophic sealevel rise and ice-sheet collapse. *Geology* **23,** 4–8.

Bradley, R. S., and Jones, P. D. (1993). 'Little Ice Age' summer temperature variations: Nature and relevance. *The Holocene* **3,** 367–376.

Braziunas, T. F. (1990). Nature and origin of variations in late-Glacial and Holocene atmospheric ^{14}C as revealed by global carbon cycle modeling. Ph.D. dissertation, Univ. of Washington.

Broecker, W. S., and Denton, G. (1989). The role of ocean-atmosphere reorganizations in glacial cycles. *Geochimica et Cosmochimica Acta* **53,** 2465–2501.

Charles, C. D., Rind, D., Jouzel, J., Koster, R. D., and Fairbanks, R. G. (1994). Glacial–interglacial changes in moisture sources for Greenland: Influences on the ice core record of climate. *Science* **263,** 508–511.

Clausen, H. B., Gundestrup, N. S., and Johnson, S. J. (1988). Glaciological investigations in the Crête area, Central Greenland: A search for a new deep-drilling site. *Annals of Glaciology* **10,** 10–15.

Cuffey, K. M., Alley, R. B., Grootes, P. M., Bolzan, J. M., and Anandakrishan, S. (1994). Calibration of the $\delta^{18}O$ isotopic paleothermometer for central Greenland, using borehole temperatures. *Journal of Glaciology* **40**(135), 341–349.

Cuffey, K. M., Clow, G. D., Alley, R. B., Stuiver, M., and Waddington, E. D., and Saltus, R. W. (in press). Large arctic temperature change at the Glacial–Holocene transition. *Science.*

Cutler, N. N., Raymond, C. F., Waddington, E. D., Meese, D. A., and Alley, R. B. (in press). The effect of ice sheet thickness change on the accumulation history inferred from GISP2 layer thicknesses. *Annals of Glaciology.*

Damon, P. E., and Sonett, C. P. (1991). Solar and terrestrial components of the atmospheric ^{14}C variation spectrum. *In* "The Sun in Time" (C. P. Sonett, M. S. Giampa, and M. S. Matthews, Eds.), pp. 360–388. Univ. of Arizona Press, Tucson, AZ.

Dansgaard, W., Johnsen, S. J., Clausen, H. B., and Gundestrup, N. (1973). Stable isotope glaciology. *Meddelelser om Grønland* **197**(2), 1–53.

Dansgaard, W., Johnsen, S. J., Clausen, H. B., Dahl-Jensen, N., Gundestrup, N., and Hammer, C. U. (1984). North Atlantic climatic oscillations revealed by deep Greenland ice cores. *In* "Climate Processes and Climate Sensitivity" (J. E. Hansen and T. Takahashi, Eds.), Geophysical Monographs 29, pp. 288–298.

Dansgaard, W., Johnsen, S. J., Clausen, H. B., Dahl-Jensen, D., Gundestrup, N. S., Hammer, C. U., Hvidberg, C. S., Steffensen, J. P., Sveinbjörnsdottir, A. E., Jouzel, J., and Bond, G. (1993). Evidence for general instability of past climate from a 250-kyr ice-core record. *Nature* **364,** 218–220.

Eddy, J. A. (1976). The Maunder minimum. *Science* **192,** 1189–1202.

Edwards, R. L., Beck, J. W., Burr, G. S., Donahue, D. J., Chappell, J. M. A., Bloom, A. L., Druffel, E. R. M., and Taylor, F. W. (1993). A large drop in atmospheric $^{14}C/^{12}C$ and reduced melting in the Younger Dryas, documented with ^{230}Th ages of corals. *Science* **260,** 962–968.

Fairbanks, R. B., Charles, C. D., and Wright, J. D. (1992). Origin of global meltwater pulses. *In* "Radiocarbon After Four Decades" (R. E. Taylor, A. Long, and R. S. Kra, Eds.), pp. 473–500. Springer-Verlag, New York.

Grootes, P. M., Stuiver, M., White, J. W. C., Johnsen, S., and Jouzel, J. (1993). Comparison of oxygen isotope records from the GISP2 and GRIP Greenland ice cores. *Nature* **366,** 552–554.

Gundestrup, N. S., Dahl-Jensen, D., Johnson, S. J., and Rossi, A. (1993). Borehole survey at dome GRIP 1991. *Cold Regions Science and Technology* **21,** 399–402.

Hammer, C. U. (1982). The history of atmospheric composition as recorded in ice sheets. *In* "Atmospheric Chemistry" (E. D. Goldberg, Eds.), Report of Dahlem Workshop, Berlin, pp. 119–134. Springer-Verlag, Heidelberg.

Johnsen, S. J., Clausen, H. B., Dansgaard, W., Fuhrer, K., Gundestrup, N., Hammer, C. U., Iversen, P., Jouzel, J., Stauffer, B., and Steffensen, J. P. (1992). Irregular glacial interstadials recorded in a new Greenland ice core. *Nature* **359,** 311–313.

Johnsen, S. J., and Robin, G. de Q. (1983). Diffusion of stable isotopes. *In* "The Climatic Record in Polar Ice Sheets" (G. de Q. Robin, Ed.), pp. 57–63. Cambridge Univ. Press, Cambridge, UK.

Kapsner, W. R., Alley, R. B., Shuman, C. A., Anandakrishnan, S., and Grootes, P. M. (1995). Dominant influence of atmospheric circulation on snow accumulation in Greenland over the past 18,000 years. *Nature* **373,** 52–54.

Kutzbach, J. E., and Webb, T. (1993). Conceptual basis for understanding Late-Quaternary climates. *In* "Global Climates since the Last Glacial Maximum," (H. E. Wright, J. E. Kutzbach, T. Webb, W. F. Ruddiman, F. A. Street-Perrott, and P. J. Bartlein, Eds.), pp. 5–11. Univ. of Minnesota Press, Minneapolis.

Labitzke, K., and van Loon, H. (1988). Associations between the 11-year solar cycle, the QBO and the atmosphere. Part I: The troposphere and stratosphere in the northern hemisphere in winter. *Journal of Atmospheric and Terrestrial Physic* **50,** 197–206.

Lamb, H. H. (1977). "Climate: Present, Past and Future. Vol. 2 Climatic History and the Future," pp. 453–454. Methuen, London.

Lehman, S. J., and Keigwin, L. D. (1992). Sudden changes in North Atlantic circulation during the last deglaciation. *Nature* **356,** 757–762.

Lingenfelter, R. E. (1963). Production of carbon 14 by cosmic-ray neutrons. *Reviews of Geophysics* **1,** 35–55.

Mangerud, J., Andersen, S. T., Berglund, B. E., and Donner, J. J. (1974). Quaternary stratigraphy of Norden, a proposal for terminology and classification. *Boreas* **3,** 109–128.

Mayewski, P. A., Meeker, L. D., Whitlow, S., Twickler, M. S., Morrison, M. C., Bloomfield, P., Bond, G. C., Alley, R. B., Gow, A. J., Grootes, P. M., Meese, D. A., Ram, M., Taylor, K. C., and Wumkes, W. (1994). Changes in atmospheric circulation and ocean ice cover over the North Atlantic during the last 41,000 years. *Science* **263,** 1747–1751.

Mazaud, A., Laj, C., Bard, E., Arnold, M., and Tric, E. (1991). Geomagnetic field control of ^{14}C production over the last 80 ky: Implications for the radiocarbon time-scale. *Geophysical Research Letters* **18,** 1885–1888.

McElhinny, M. W., and Senanayake, W. E. (1982). Variations in the geomagnetic dipole 1: The past 50,000 years. *Journal of Geomagnetism and Geoelectricity* **34,** 39–51.

Meese, D. A., Alley, R. B., Gow, A. J., Grootes, P. M., Mayewski, P. A., Ram, M., Taylor, K. C., Waddington, I. E., and Zielinski, G. A. (1994a). "Preliminary Depth-Age Scale of the GISP2 Ice Core," CRREL Special Report 94-1, 66 p.

Meese, D. A., Gow, A. J., Grootes, P. M., Mayewski, P. A., Ram, M., Stuiver, M., Taylor, K. C., Waddington, E. D., and Zielinski, G. A. (1994b). The accumulation record from the GISP2 core as an indicator of climate change throughout the Holocene. *Science* **266,** 1680–1682.

Newhall, C. G., and Self, S. (1982). The volcanic explosivity index (VEI): An estimate of explosive magnitude for historical volcanism. *Journal of Geophysical Research* **87,** 1231–1238.

Nilsson, T. (1983). "The Pleistocene, Geology and Life in the Quaternary Ice Age." Reidel, Dordrecht.

O'Brien, K. (1979). Secular variations in the production of cosmogenic isotopes. *Journal of Geophysical Research* **84,** 423–431.

O'Brien, D. P., and Currie, R. G. (1993). Observations of the 18.6-year cycle of air pressure and a theoretical model to explain certain aspects of this signal. *Climate Dynamics* **8,** 287–298.

Ogilvie, A. E. J. (1984). The past climate and sea-ice record from Iceland, Part I: Data to A.D. 1780. *Climatic Change* **6,** 131–152.

Quinn, W. H., and Neal, V. T. (1992). The historical record of El Nino events. *In* "Climate Since AD 1500, London and New York" (R. S. Bradley and P. D. Jones, Eds.), pp. 623–648. Routledge/Chapman and Hall, London.

Schatten, K. H. (1988). A model for solar constant secular changes. *Geophysical Research Letters* **15,** 121–124.

Schlesinger, M. E., and Ramankutty, N. (1994). An oscillation in the global climate system of period 65–70 years. *Nature* **367,** 723–726.

Shuman, C. A., Alley, R. B., Anandakrishnan, S., White, J. W. C., Grootes, P. M., and Stearns, C. R. (in press). Temperature and accumulation at the Greenland Summit: Comparison of high-resolution isotope profiles and satellite passive microwave brightness temperature trends. *Journal of Geophysical Research.*

Steig, E. J., Grootes, P. M., and Stuiver, M. (1994). Seasonal precipitation timing and ice core records. *Science* **266,** 1885–1886.

Stothers, R. B. (1989). Volcanic eruptions and solar activity. *Journal of Geophysical Research* **94,** 17371–17381.

Stuiver, M., and Braziunas, T. F. (1993). Sun, ocean, climate and atmospheric $^{14}CO_2$: An evaluation of causal and spectral relationships. *The Holocene* **3,** 289–305.

Stuiver, M., Braziunas, T. F., Becker, B., and Kromer, B. (1991). Climatic, solar, oceanic, and geomagnetic influences on Late-glacial and Holocene atmospheric $^{14}C/^{12}C$ change. *Quaternary Research* **35,** 1–24.

Stuiver, M., and Polach, H. A. (1977). Discussion: Reporting of ^{14}C data. *Radiocarbon* **19,** 355–363.

Stuiver, M., and Quay, P. D. (1980). Changes in atmospheric carbon-14 attributed to a variable sun. *Science* **207,** 11–19.

Stuiver, M., Quay, P. D., and Braziunas, T. F. (in press). Isotope and carbon cycle inferences. *In* "Proceeding, Global Change Institute The Carbon Cycle, Snowmass, July 1993, UCAR, Boulder."

Stuiver, M., and Reimer, P. J. (1993). Extended ^{14}C data base and revised CALIB 3.0 ^{14}C age calibration program. *Radiocarbon* **35,** 215–230.

Van Loon, H., and Labitzke, K. (1988). Association between the 11-year solar cycle, the QBO, and the atmosphere. Part II: Surface and 700 mb in the Northern Hemisphere in winter. *Journal of Climate* **1,** 905–920.

Whillans, I. M., and Grootes, P. M. (1985). Isotope diffusion in cold snow and firn. *Journal of Geophysical Research* **90,** 3910–3918.

Wilson, R. C., and Hudson, H. S. (1988). Solar luminosity variations in solar cycle 21. *Nature* **332,** 810–812.

Zielinski, G. A., Mayewski, P. A., Meeker, L. D., Whitlow, S., Twickler, M. S., Morrison, M., Meese, D. A., Gow, A. J., and Alley, R. B. (1994). Record of volcanism since 7000 B.C. from the GISP2 Greenland ice core and implications for the volcano-climate system. *Science* **264,** 948–952.